

Nuclear response beyond the Fermi gas model

Omar Benhar

INFN, Sezione di Roma, and Department of Physics, Università “La Sapienza”
Piazzale Aldo Moro, 2. I-00185 Roma, Italy

The Fermi gas model, while providing a reasonable qualitative description of the continuum nuclear response, does not include the effects of dynamical nucleon-nucleon correlations in the initial and final states, that have long been recognized to play a critical role in specific kinematical regions. We review a many-body approach in which these effects are consistently taken into account and discuss the results of a calculation of the quasielastic neutrino-oxygen cross section as an illustrative example.

1. Introduction

Within the Fermi gas (FG) model the nucleus is seen as a degenerate gas of protons and neutrons at density ρ , binding effects being taken into account through the inclusion of an average interaction energy $\bar{\epsilon}$ [1].

In spite of its simplicity, the FG model provides a remarkably good description of the inclusive electron-nucleus cross section in the region of the quasi free peak, corresponding to $x_B = Q^2/2m\nu \sim 1$, where x_B is the Bjorken scaling variable, $Q^2 = \mathbf{q}^2 - \nu^2$, \mathbf{q} and ν being the momentum and energy transfer, respectively, and m denotes the nucleon mass. The successful application to the analysis of electron scattering data at moderate momentum transfer ($\mathbf{q} \sim 150 - 200$ MeV) [2] also prompted the extension of the FG approach to the case of neutrino-nucleus scattering [3].

Over the past two decades the limitations of the FG description have been exposed by the growing availability of new electron scattering data, extending into the region of large \mathbf{q} and low ν , corresponding to $x_B \gg 1$. The failure of the FG model to explain the measured cross sections in this kinematical regime, clearly illustrated in Fig. 1, has been ascribed to the dominance of scattering off nucleons belonging to *strongly correlated* pairs, that cannot be accounted for by any mean field approach.

In addition, it has to be pointed out that, as

the FG model does not include surface and shell effects, it cannot be employed to study exclusive channels, which are known to be sensitive to the details of the nuclear wave function.

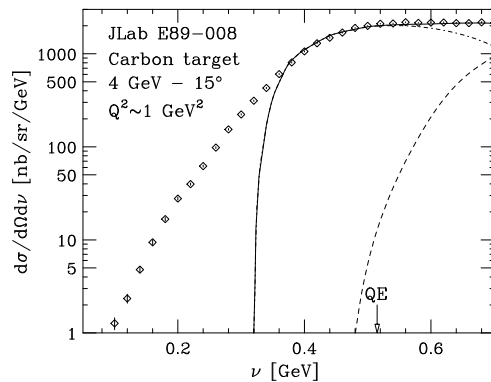


Figure 1. Cross section versus energy loss for scattering of 4 GeV electrons at 15° from Carbon. The dot-dash, dashed and full lines show the quasielastic, inelastic and total cross sections predicted by the FG model with $k_F = 221$ MeV and $\bar{\epsilon} = 35$ MeV. The arrow points to the value of ν corresponding to quasi-free kinematics. The experimental data are taken from ref. [4].

In this paper we review a theoretical approach, based on nonrelativistic nuclear many-body theory, that incorporates in a consistent fashion

dynamical nucleon-nucleon (NN) correlations in both the initial and final state. The impulse approximation (IA) scheme, which allows one to relate the cross section to the nuclear spectral function $P(\mathbf{p}, E)$, describing the energy-momentum distributions of nucleons in the target nucleus, is outlined in Section 2. The main features of $P(\mathbf{p}, E)$, extracted from both experiments and theoretical calculations, are described in Section 3, while Section 4 is devoted to the discussion of final state interactions (FSI). Finally, in Section 5 we summarize the results and state the conclusions.

2. The impulse approximation

The main assumption underlying IA is that, as the space resolution of a probe delivering momentum \mathbf{q} to a nucleus is $\sim 1/|\mathbf{q}|$, at large enough $|\mathbf{q}|$ the target is seen by the probe as a collection of individual nucleons. Within this picture, the nuclear response measures the probability that, after giving one nucleon a momentum \mathbf{q} at time $t = 0$, the system be reverted to the ground state giving the *same* particle a momentum $-\mathbf{q}$ after time t .

The second assumption involved in IA is that (FSI) taking place at $0 < t' < t$ between the hit nucleon and the (A-1)-nucleon spectator system be negligible.

In the IA regime the scattering process off a nuclear target reduces to the incoherent sum of elementary processes involving only one nucleon, as schematically illustrated in Fig. 2.

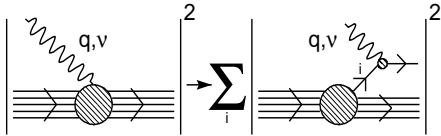


Figure 2. Pictorial representation of the IA scheme, in which the nuclear cross section is replaced by the incoherent sum of cross sections describing scattering off individual nucleons, the recoiling (A-1)-particle system acting as a spectator.

Let us consider the weak charged current reaction

$$\nu_\mu + A \rightarrow \mu^- + p + (A - 1) . \quad (1)$$

According to IA, the corresponding differential cross section can be written

$$\frac{d\sigma_{IA}}{d\Omega_\mu dE_\mu} = \int d^3p dE P(\mathbf{p}, E) \frac{d\sigma_N}{d\Omega_\mu dE_\mu} \times \delta(E_\nu - E_\mu - E - E_{\mathbf{p}'}) , \quad (2)$$

where $d\sigma_N/d\Omega_\mu dE_\mu$ is the cross section describing the elementary scattering process

$$\nu_\mu(k) + n(p) \rightarrow \mu^-(k') + p(p') , \quad (3)$$

involving a *bound* nucleon carrying momentum \mathbf{p} . The spectral function $P(\mathbf{p}, E)$, yielding the probability of removing a nucleon with momentum \mathbf{p} from the nuclear ground state leaving the residual system with excitation energy E , will be discussed in Section 3.

Up to a kinematical factor, the elementary cross section reads

$$\frac{d\sigma_N}{d\Omega_\mu dE_\mu} \propto \frac{G^2}{2} L_{\mu\nu}(k, k') W^{\mu\nu}(p, \tilde{q}) , \quad (4)$$

where $G = G_F \cos\theta_c$, G_F and θ_c being Fermi's coupling constant and Cabibbo's angle, respectively. The lepton tensor $L_{\mu\nu}$ is totally specified by kinematical variables, whereas the definition of $W^{\mu\nu}(p, \tilde{q})$, describing the weak interactions of a *free* nucleon, involves the Dirac, Pauli and axial form factors F_1 , F_2 and F_A .

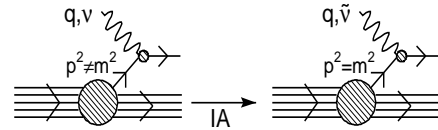


Figure 3. Schematic representation of the IA treatment of the lepton nucleon vertex. The elementary scattering amplitude is assumed to be the same as in free space, binding effects being taken into account replacing the energy transfer ν with $\tilde{\nu}$ (see text).

Within the IA scheme binding is taken into account replacing the physical four-momentum transfer $q = k - k' \equiv (\nu, \mathbf{q})$ with $\tilde{q} \equiv (\tilde{\nu}, \mathbf{q})$, where

$$\tilde{\nu} = \nu + M_A - \sqrt{|\mathbf{p}|^2 + M_{A-1}^2} - \sqrt{|\mathbf{p}|^2 + m^2}, \quad (5)$$

M_A and $M_{A-1} = M_A - m + E$ being the target mass and the mass of the recoiling nucleus, respectively [5]. This essentially amounts to assuming that: i) a fraction $(\nu - \tilde{\nu})/\nu$ of the lepton energy loss is spent to put the struck nucleon on the mass shell and ii) the elementary scattering process can be described as if it took place in free space with energy transfer $\tilde{\nu} < \nu$.

3. The nuclear spectral function

Let us consider a system of A nucleons whose dynamics is described by the nonrelativistic hamiltonian

$$H_A = \sum_{i=1}^A \frac{\mathbf{p}_i^2}{2m} + \sum_{j>i=1}^A v_{ij} + \dots, \quad (6)$$

where \mathbf{p}_i is the momentum of the i -th nucleon, v_{ij} is the NN potential and the ellipsis indicates the presence of three-nucleon interactions¹.

The spectral function is defined as (see, e.g., ref. [6])

$$P(\mathbf{p}, E) = \sum_n \left| \langle \Psi_n^{(A-1)} | a_{\mathbf{p}} | \Psi_0^A \rangle \right|^2 \times \delta(E + E_0 - E_n), \quad (7)$$

where $|\Psi_0^A\rangle$ is the nuclear ground state, satisfying the Schrödinger equation $H_A |\Psi_0^A\rangle = E_0 |\Psi_0^A\rangle$, while $|\Psi_n^{(A-1)}\rangle$ and E_n denote the n -th eigenstate of the $(A-1)$ -nucleon system and the associated energy eigenvalue, respectively.

Due to the complex spectrum of $(A-1)$ -nucleon states, in general the calculation of $P(\mathbf{p}, E)$ within nuclear many-body theory involves prohibitive difficulties. It has been carried out only for few-nucleon systems, having $A = 3$ [7,8] and 4 [9], and uniform symmetric nuclear matter, i.e. in the limit $A \rightarrow \infty$ with $Z=A/2$ [6,10].

¹The inclusion of a three-nucleon potential in nuclear many-body theory is needed to reproduce the binding energy of the three-nucleon system and the empirical equilibrium density of nuclear matter.

Spectral functions of nuclei with $A > 4$ have been constructed using the Local Density Approximation (LDA) [11]. Within this approach $P(\mathbf{p}, E)$ is split into two parts, corresponding to low momentum nucleons, sitting in single particle shell model states, and high-momentum nucleons, belonging to strongly correlated pairs, respectively.

The spectral function of the shell model states has been extensively measured by single nucleon knock-out experiments (see, e.g., ref. [12]), whereas the correlation part is obtained from the results of theoretical calculations through [11]

$$P_{corr}(\mathbf{p}, E) = \int d^3r \rho(\mathbf{r}) P_{corr}^{NM}(\mathbf{p}, E; \rho(\mathbf{r})) \quad (8)$$

where $\rho(\mathbf{r})$ is the nuclear density distribution and $P_{corr}^{NM}(\mathbf{p}, E; \rho)$ is the correlation part of the spectral function of infinite nuclear matter at uniform density ρ .

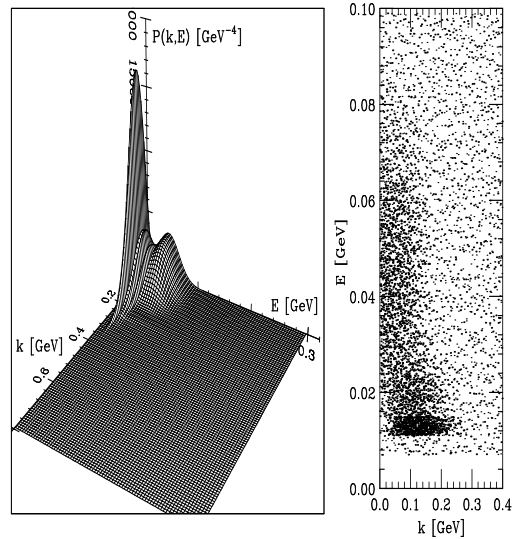


Figure 4. Three-dimensional plot (left panel) and scatter plot (right panel) of the oxygen spectral function obtained using the LDA approximation described in the text.

The LDA spectral function of ^{16}O obtained combining the nuclear matter results of ref. [6]

and the Saclay ($e, e'p$) data [13] is shown in Fig. 4. The shell model states account for $\sim 80\%$ of the strength, whereas the remaining $\sim 20\%$ is located at high momentum ($|\mathbf{p}| \gg k_F$) and large removal energy ($E \gg E_F$, where E_F denotes the Fermi energy). It has to be emphasized that large E and large \mathbf{p} are strongly correlated. For example, $\sim 50\%$ of the strength at $|\mathbf{p}| = 320$ MeV is located at $E > 80$ MeV.

Fig. 5 shows the momentum distribution of nucleons in the ground state of ^{16}O , obtained from the LDA spectral function through

$$n(\mathbf{p}) = \int dE P(\mathbf{p}, E) . \quad (9)$$

Comparison with the results of a Monte Carlo calculation carried out using a highly realistic many-body wave function [14] suggests that LDA results are quite reasonable. For reference, the Fermi gas momentum distribution corresponding to $k_F = 220$ MeV is also shown by the dashed line.

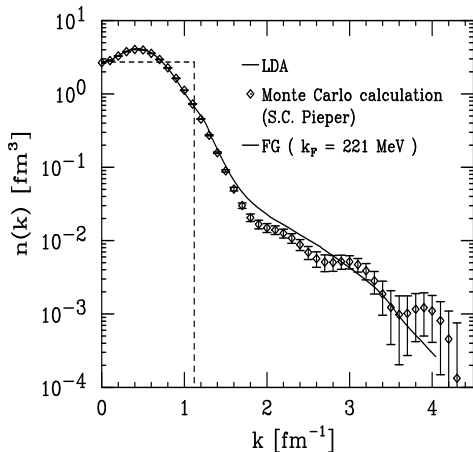


Figure 5. Momentum distribution of nucleons in the oxygen ground state. Solid line: LDA approximation. Dashed line: Fermi gas model with $k_F = 220$ MeV. Diamonds: Monte Carlo calculation carried out by S.C. Pieper using the wave function of ref. [14].

The lepton energy loss dependence of the calculated cross section of the process $\nu_\mu + ^{16}\text{O} \rightarrow$

$\mu^- + p + X$ is displayed in Fig. 6 for the case of neutrino energy $E_\nu = 2$ GeV and muon scattering angle 30° . Comparison between the solid line, obtained using the LDA spectral function, and the dashed line, corresponding to the FG model, shows that the inclusion of dynamical NN correlations produces a quenching of the peak associated with the appearance of sizeable tails, particularly at large lepton energy loss.

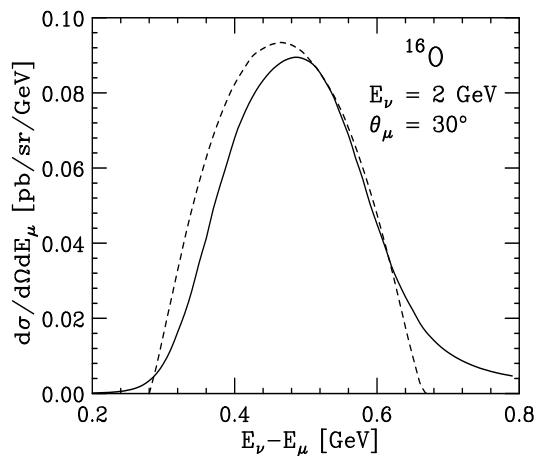


Figure 6. Cross section of the process $\nu_\mu + ^{16}\text{O} \rightarrow \mu^- + p + X$. Solid line: IA calculation carried out using the LDA spectral function discussed in the text. Dashed line: Fermi gas model with $k_F = 220$ MeV and $\bar{\epsilon} = 25$ MeV.

The presence of high-momentum and high-energy components in the nuclear wave function is also responsible for the shift in the position of the peaks. The average removal energy

$$\langle E \rangle = \int d^3p dE EP(\mathbf{p}, E) , \quad (10)$$

calculated using the LDA spectral function of ^{16}O , $\langle E \rangle = 42$ MeV, is in fact much larger than the binding energy $\bar{\epsilon} = 25$ MeV of the FG model.

4. Final state interactions

The occurrence of FSI leads to the breakdown of the IA picture of the scattering process, thus

making the reconstruction of its kinematics much more difficult.

A number of theoretical studies of FSI in $(e, e'p)$ have been carried out within the Distorted Wave Impulse Approximation [15], in which the spectral function is modified to take into account the distortion of the struck nucleon wave function produced by its interactions with the spectators, described by a complex optical potential. DWIA has been successfully employed to analyze two-body breakup processes, in which the spectator system is left in a bound state, for proton energies $\lesssim 100$ MeV.

Realistic many-body calculations of nuclear structure provide strong *a priori* indication that the PWIA picture is not likely to be applicable even at much larger energies.

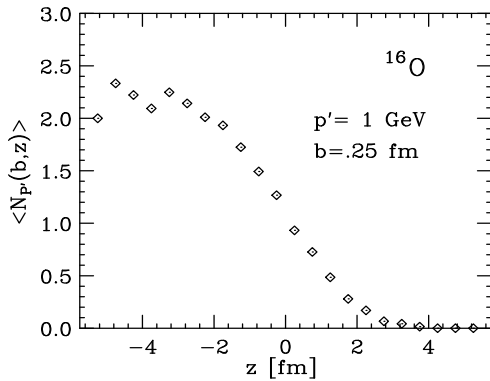


Figure 7. The function $\langle N_{\mathbf{p}'}(\mathbf{b}, z) \rangle$, defined by Eq.(11), plotted at $b = 0.25$ fm for a 1 GeV nucleon knocked out from oxygen.

The probability that a nucleon hit at position \mathbf{r} in the target center of mass frame and left with momentum \mathbf{p}' in the direction of the z -axis rescatter against the spectator particles is illustrated in Fig. 7, showing the z -dependence of the quantity

$$\langle N_{\mathbf{p}'}(\mathbf{b}, z) \rangle = \frac{1}{\rho(\mathbf{r})} \int dR |\Psi_0(R)|^2 \sum_{i=1}^A \delta(\mathbf{r} - \mathbf{r}_i) \times \sum_{j \neq i=1}^A \theta \left(\sqrt{\frac{\sigma_{NN}(\mathbf{p}')}{\pi}} - |\mathbf{b} - \mathbf{b}_j| \right) \theta(z_j - z), \quad (11)$$

evaluated at $|\mathbf{b}| = \sqrt{|\mathbf{r}|^2 - z^2} = 0.25$ fm for the case of a 1 GeV nucleon knocked out from oxygen. In Eq.(11) $\rho(\mathbf{r})$ and $\Psi_0(R)$, with $R \equiv (\mathbf{r}_1, \dots, \mathbf{r}_A)$, denote the target density and ground state wave function, respectively, whereas $\sigma_{NN}(\mathbf{p}')$ is the NN scattering cross section at incident momentum \mathbf{p}' . The 3A-dimensional integral has been carried out using Monte Carlo configurations sampled from the probability distribution associated with the ^{16}O wave function of ref. [14].

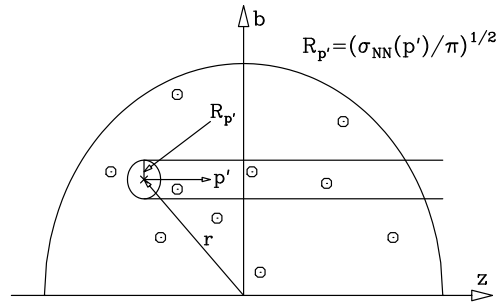


Figure 8. Schematic representation of rescattering in nucleon knock-out processes.

The quantity $\langle N_{\mathbf{p}'}(\mathbf{b}, z) \rangle$ is the average number of spectators found within the cylindrical volume described by a circle of area $\sigma_{NN}(\mathbf{p}')$ initially centered at \mathbf{r} and moving along the direction of the momentum \mathbf{p}' (see Fig. 8). Its value provides an estimate of the number of rescatterings undergone by the knocked out particle. The results shown in Fig. 7 suggest that in the case of scattering processes involving nucleons in the $z < 0$ hemisphere, the struck particle is likely to interact with at least one of the spectators.

A theoretical treatment of the corrections to the IA cross section due to FSI effects was developed in ref. [16] and extensively applied to the analysis of inclusive electron-nucleus scattering data [9,11,16]. The main approximations involved in the approach of ref. [16], expected to be reasonable at large \mathbf{p}' , are that i) the struck particle moves along a straight trajectory with a constant velocity \mathbf{v} (*eikonal approximation*) and ii) the spectator particles are seen by the fast struck

nucleon as a collection of fixed scattering centers (*frozen approximation*).

Under the above assumptions the ground state averaged propagator of the struck nucleon can be written in the factorized form

$$U_{\mathbf{p}'}(t) = U_{\mathbf{p}'}^0(t)U_{\mathbf{p}'}^{FSI}(t), \quad (12)$$

where $U_{\mathbf{p}'}^0$ is the free space propagator, while FSI effects are described by the quantity

$$U_{\mathbf{p}'}^{FSI}(t) = \left\langle \frac{1}{A} \sum_{i=1}^A e^{i \sum_{j \neq i} \int_0^t dt' w_{\mathbf{p}'}(|\mathbf{r}_{ij} + \mathbf{v}t'|)} \right\rangle. \quad (13)$$

In Eq.(13) $\mathbf{r}_{ij} = \mathbf{r}_i - \mathbf{r}_j$, $w_{\mathbf{p}'}(|\mathbf{r}|)$ is the coordinate-space NN scattering t-matrix, parametrized in terms of total cross section, slope and real to imaginary part ratio, and $\langle \dots \rangle$ denotes the expectation value in the target ground state.

Note that $U_{\mathbf{p}'}^{FSI}(t)$ is simply related to the nuclear transparency $T_{\mathbf{p}'}$, measured in coincidence ($e, e'p$) experiments [17], through

$$T_{\mathbf{p}'} = \lim_{t \rightarrow \infty} |U_{\mathbf{p}'}^{FSI}(t)|^2. \quad (14)$$

In presence of FSI the inclusive cross section can still be expressed in terms of the IA result of Eq.(2) through [16]

$$\frac{d\sigma}{d\Omega_\mu dE_\mu} = \int dE'_\mu \frac{d\sigma_{IA}}{d\Omega_\mu dE'_\mu} f_{\mathbf{p}'}(E_\mu - E'_\mu), \quad (15)$$

the folding function $f_{\mathbf{p}'}(\omega)$ being defined as

$$f_{\mathbf{p}'}(\omega) = \delta(\omega)T_{\mathbf{p}'}^{1/2} + \int \frac{dt}{2\pi} e^{i\omega t} \left[U_{\mathbf{p}'}^{FSI}(t) - T_{\mathbf{p}'}^{1/2} \right]. \quad (16)$$

The above equations clearly show that the strength of FSI is measured by both $T_{\mathbf{p}'}$ and the width of the folding function. In absence of FSI $U_{\mathbf{p}'}^{FSI}(t) \equiv 1$, implying in turn $T_{\mathbf{p}'} = 1$ and $f_{\mathbf{p}'}(\omega) \rightarrow \delta(\omega)$.

Fig. 9 shows the quantity $f_{\mathbf{p}'}(\omega) - \delta(\omega)T_{\mathbf{p}'}^{1/2}$, evaluated for a 1 GeV nucleon knocked out from oxygen using a parametrization of the measured NN scattering amplitude [18] and the wave function of ref. [14].

The effect of FSI on the calculated cross section of the process $\nu_\mu + {}^{16}\text{O} \rightarrow \mu^- + p + X$ at neutrino

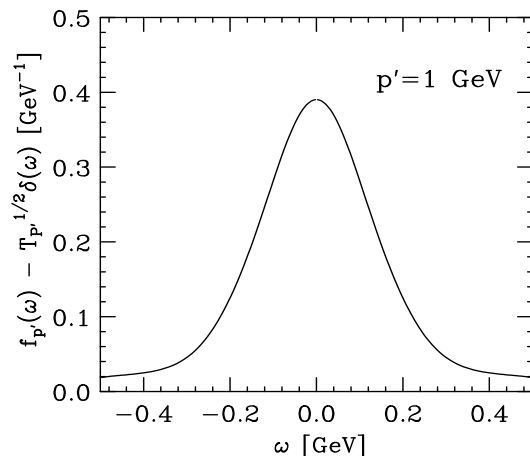


Figure 9. Finite width contribution to the folding function of Eq.(16), evaluated for a 1 GeV nucleon knocked out from oxygen using a parametrization of the measured NN scattering amplitude [18] and the wave function of ref. [14].

energy $E_\nu = 2$ GeV and muon scattering angle 30° is illustrated in Fig. 10. It clearly appears that, in spite of the fact that the finite width component contributes only $\sim 15\%$ of the folding function normalization, the inclusion of FSI produces a sizable redistribution of the strength, resulting in a quenching of the peak and an enhancement of the tails.

5. Summary and conclusions

Nuclear many-body theory provides a consistent framework allowing for a description of the continuum nuclear response that takes into account dynamical effects not included in the FG model.

The approach discussed in this paper, that has been extensively applied to the analysis of electron-nucleus scattering data, is based on the IA picture, in which the lepton probe scatters off individual nucleons distributed in momentum and energy according to the spectral function $P(\mathbf{p}, E)$.

While this picture proved to work exceedingly well for scattering of few GeV electrons, its appli-

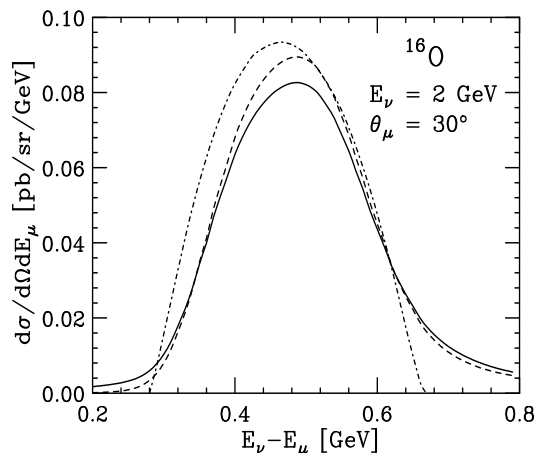


Figure 10. Cross section of the process $\nu + {}^{16}\text{O} \rightarrow \mu + p + X$. Solid line: Full calculation, including FSI. Dashed line: IA calculation. Dot-dash line: Fermi gas model with $k_F = 220$ MeV and $\bar{\epsilon} = 25$ MeV.

capability in the region of lower energies relevant to neutrino experiments needs to be quantitatively investigated. For example, the effect of Pauli blocking of the struck nucleon is likely to play a non negligible role at $E_\nu \lesssim 700$ MeV.

Comparison between the results of the FG model and those obtained using a realistic spectral function shows that the inclusion of dynamical correlation effects, leading to the appearance of high momentum and high removal energy components, sizably affects the response.

Corrections to the IA cross sections due to the occurrence of FSI, which have long been recognized to play a major role in redistributing the inclusive strength, can also be taken into account in a consistent fashion within nuclear many-body theory.

As a final remark, it is worthwhile mentioning that the proposed many-body approach can be readily generalized to include the contribution of inelastic channels in a fully consistent fashion.

Acknowledgments

The author would like to thank Steven Pieper

for providing the Monte Carlo configurations employed in the calculation of FSI effects. Many illuminating discussions with Adelchi Fabrocini, Stefano Fantoni, Vijay Pandharipande and Ingo Sick are also gratefully acknowledged.

REFERENCES

1. E.J. Moniz, Phys. Rev. 184 (1969) 1154.
2. E.J. Moniz *et al*, Phys. Rev. Lett. 26 (1971) 445.
3. R.A. Smith and E.J. Moniz, Nucl. Phys. B43 (1972) 605.
4. J. Arrington *et al*, Phys. Rev. Lett. 82 (1999) 2056.
5. T. de Forest, Jr., Nucl. Phys. A392 (1983) 232.
6. O. Benhar, A. Fabrocini and S. Fantoni, Nucl. Phys. A505 (1989) 267.
7. C. Ciofi degli Atti, E. Pace and G. Salmè, Phys. Rev. C 21 (1980) 805.
8. H. Meier-Hajduk, Ch. Hadjuk and P.U. Sauer, Nucl. Phys. A395 (1983) 332.
9. O. Benhar and V.R. Pandharipande, Phys. Rev. C 47 (1993) 2218.
10. A. Ramos, A. Polls and W.H. Dickhoff, Nucl. Phys. A503 (1989) 1.
11. O. Benhar, A. Fabrocini, S. Fantoni and I. Sick, Nucl. Phys. A579 (1994) 493.
12. *Modern Topics in Electron Scattering*, Eds. B. Frois and I. Sick (World Scientific, Singapore, 1991).
13. S. Turck-Chièze, Lecture Notes in Physics, 137 (1981) 251.
14. S.C. Pieper, R.B. Wiringa and V.R. Pandharipande, Phys. Rev. C 46 (1992) 1741.
15. S. Boffi, C. Giusti and F.D. Pacati, Phys. Rep. 226 (1993) 1.
16. O. Benhar *et al*, Phys. Rev. C 44 (1991) 2328.
17. D. Abbott *et al*, Phys. Rev. Lett. 80 (1998) 5072.
18. T.G. O'Neill, private communication.